Continuous Culture of the budding yeast strain IFO 0233

Calculation of metabolic exchange rates

Rainer Machné and Douglas B. Murray

June 10, 2025

Pre-Culture *Saccharomyces cerevisiae* (strain IFO 0233) were maintained on yeast nitrogen base agar plates ($2\,\%$ glucose, $1.5\,\%$ agar; Difco, Japan) at $4\,^{\circ}\mathrm{C}$, sub-cultured from frozen stock cultures (-$80\,^{\circ}\mathrm{C}$; $1\,\mathrm{mL}$; $15\,\%$ glycerol; 5×10^8 cells). Pre-cultures were inoculated into Yeast Extract Peptone Dextrose media ($10\,\mathrm{mL}$; $1\,\%$ yeast extract, $2\,\%$ peptone, $2\,\%$ glucose) and grown at $30\,^{\circ}\mathrm{C}$ in an orbital incubator ($200\,\mathrm{rpm}$) for $24\,\mathrm{h}$.

Continuous Culture Medium & Inoculation The culture medium consisted of D-glucose ($20\,\mathrm{g\,L^{-1}}$), (NH4)2SO4 ($5\,\mathrm{g\,L^{-1}}$), KH2PO4 ($2\,\mathrm{g\,L^{-1}}$), MgSO4.7H2O ($0.5\,\mathrm{g\,L^{-1}}$), CaCl2.2H2O ($0.1\,\mathrm{g\,L^{-1}}$), FeSO4.7H2O ($20\,\mathrm{mg\,L^{-1}}$), ZnSO4.7H2O ($10\,\mathrm{mg\,L^{-1}}$), CuSO4.5H2O ($5\,\mathrm{mg\,L^{-1}}$), MnCl2.4H2O ($1\,\mathrm{mg\,L^{-1}}$), $70\,\%$ H2SO4, ($1\,\mathrm{mL\,L^{-1}}$), Difco yeast extract ($1\,\mathrm{g\,L^{-1}}$) and Sigma Antifoam A ($0.2\,\mathrm{mL\,L^{-1}}$). All chemicals were supplied by Wako Pure Chemical Industries Ltd., Japan. The medium prepared with this recipe has a pH of ca. 2.5 which allows for autoclaving of media with both sugar and ammonium without browning (caramelization) and further avoids precipitation of salts in feed medium bottles during continuous culture. A custom-built bioreactor as outlined below was filled with $0.635\,\mathrm{L}$ of medium and autoclaved ($121\,^{\circ}\mathrm{C}$; $15\,\mathrm{min}$). Aeration ($0.15\,\mathrm{L\,min^{-1}}$), agitation ($750\,\mathrm{rpm}$), and temperature ($30\,^{\circ}\mathrm{C}$) and pH (3.4) control were switched on, until the system was equilibrated. Then, the dissolved oxygen probe was 2-point calibrated by flushing with pure nitrogen ($0\,\%$) and switching back to air ($100\,\%$). The equilibrated and fully calibrated reactor was inoculated with $\approx 1 \times 10^9$ pre-culture yeast cells. A batch phase continued for $\approx 40\,\mathrm{h}$ until the cells had reached stationary phase, indicated by a sharp decrease in respiratory activity. Then continuous culture, *i.e.*, feeding with fresh medium, was initiated (at $44.5\,\mathrm{h}$ in Figure 1).

Culture Control & Monitoring Continuous culture was performed in a custom-built bioreactor. The culture vessel was a jar fermentor (Eyela, Japan) with a total volume of $2.667\,\mathrm{L}$. Culture volume was measured using a balance (SB16001, Mettler Toledo, Japan), and continuous dilution with fresh medium was performed using a peristaltic pump (AC2110, ATTA, Japan) with a six roller planetary design which minimizes pulsing during rotation (about $10\,\mathrm{rpm}$), and medium was pumped through $1\,\mathrm{mm}$ tubing (inner diameter; Masterflex, Cole Palmer, USA) and a 23 gauge steel needle. This ensured that the media was introduced in a stream of <$20\,\mu\mathrm{L}$ droplets and just under a droplet per second at the operating dilution rate. Feed medium bottle weight was monitored by a balance (PMK-16, Mettler Toledo, Japan), set up to read from unstable environments and shielded from direct breezes. The culture was agitated at $750\,\mathrm{rpm}$ and aerated at $0.150\,\mathrm{L\,min^{-1}}$ by a mass flow controller (B.E. Marubishi, Japan). Dissolved oxygen was measured using an InPro 6800 sensor and pH with an InPro 3030 (both: Mettler Toledo, Japan). Culture pH was maintained at 3.4 by

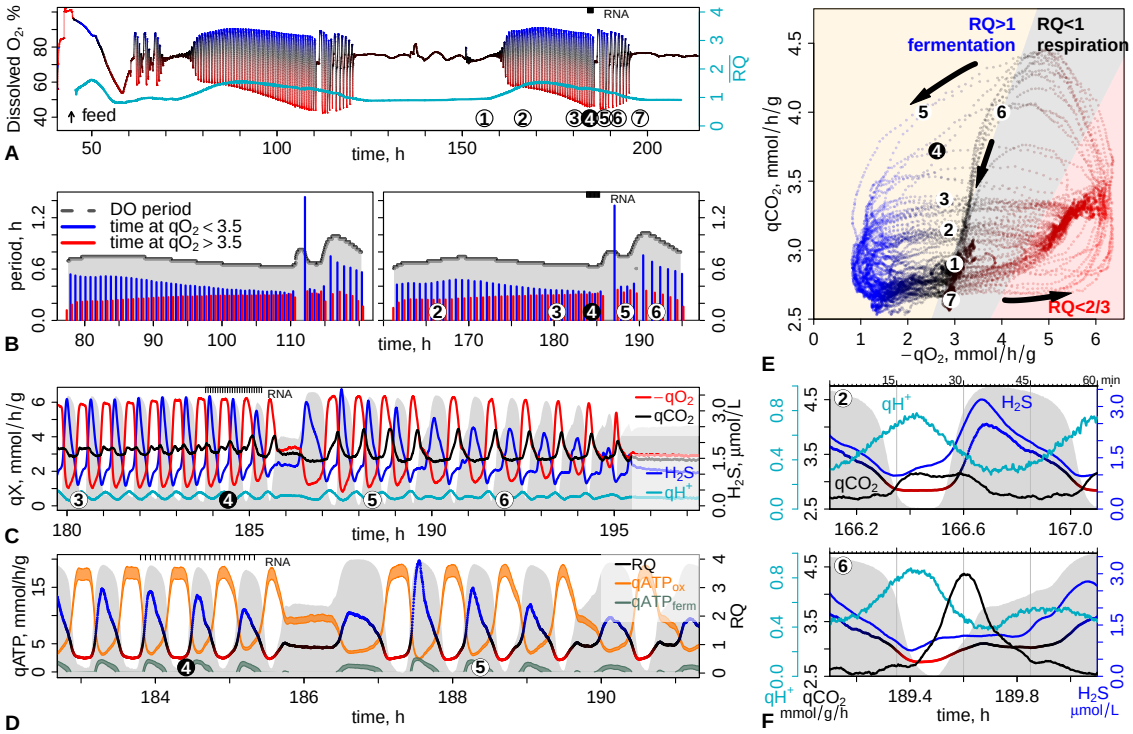

Figure 1: **Complex Dynamics: Slow Transients and a Sudden Bifurcation.** Metabolic dynamics during continuous culture of the budding yeast strain IFO 0233: panel A shows the full recorded time-series of the culture, and panels B–F zoom in on the time axis; bullet points P1–P7 serve as a guide between panels and are discussed in the text. The gray backgrounds show the dissolved O_2 concentration (see A for axis) and serves as a reference to oscillation phase. **A:** Dissolved O_2 (DO) measurement from the start of continuous feeding (dilution rate $\phi = 0.089\,\mathrm{h}^{-1}$). Line colors are derived from the respiratory quotient RQ (D) and indicate phases of high O_2 consumption (HOC: red) and low O_2 consumption (LOC: blue). The cyan line and right axis show the temporal mean $\overline{\mathrm{RQ}}$, a moving average over ca. 10 h. **B:** The cycle periods were derived from a Wavelet transform of the DO signal and the phase lengths are the time spans of each cycle where oxygen uptake ($-q_{O_2}$) stayed below (red, HOC) or above (blue, LOC) $3.5\,\mathrm{mmol/h/g_{DCW}}$. **C:** Zoom on P3–P6 for measured metabolic rates and concentrations; q_{O_2}, q_{CO_2} and H_2S were measured in the offgas of the reactor, corrected for the measurement delay and H_2S concentration was derived via its solubility. Proton export (q_{H^+}) was calculated from the NaOH addition rate. **D:** Zoom on P4–P5 for calculated rates. The respiratory quotient (RQ) and ATP production rates by respiration (q_{ATPox}) or by fermentation ($q_{ATPferm}$) were calculated from q_{O_2} and q_{CO_2} (Eq. 9–14). The RQ color gradient serves as a reference in (A, E,F). **E:** Phase portrait of q_{O_2} and q_{CO_2} over the time range indicated by bullet points in (A); points are colored by RQ (D) and in $10\,\mathrm{s}$ resolution; background colors indicate RQ ranges and arrows indicate time direction. **F:** One-hour snapshots at different times (bullet points 2 and 5). Data are indicated by colored axes and labels, except for RQ which is shown without axis but color-coded (red-black-blue) as in D and E. All reactor data is available as Datafile S1.

the automatic addition of $2.5\,\mathrm{mol\,L}^{-1}$ NaOH, and the weight of the NaOH bottle was monitored on a balance (PM400). Local control of agitation and pH was carried out by Labo controllers (B.E. Marubishi, Japan). The reactor pressure was monitored by a manometer (DM-760, Comfix, Japan) installed on a split outlet flow stream. The culture temperature was controlled at $30\,^{\circ}\mathrm{C}$ by an external sensor connected to a circulating water bath (F25-ME, Julabo, Japan). Partial pressure of oxygen and carbon dioxide in the off-gas were measured by an Enoki-III gas analyzer (Figaro

engineering, Japan). The partial pressure of hydrogen sulfide in the off-gas was measured using an electrode based gas monitor (HSC-1050HL, GASTEC, Japan). Instruments were calibrated as per manufacturer's instruction.

Reactor Data Acquisition Data were acquired *via* the in-house `FERMtastic` software at $0.1\,\mathrm{Hz}$. Metabolic rates were calculated as described previously [16, 3, 15, 5, 7] from the online recorded data. All data were processed in the script `samplingSeq_2019.R` of the `yeastSeq2016` git repository. All calculated rates are provided in Dataset S1.

Data Pre-Processing. Before all calculations some data were mildly smoothed (Fig. S1) by taking the means of moving windows of 10 measurements ($90\,\mathrm{s}$), for all offgas partial pressures ($p_{\mathsf{out}}(t)$), and of 30 measurements ($290\,\mathrm{s}$) for the culture and water bath temperatures ($T(t)$ and $T_{\mathsf{b}}(t)$). This was required to avoid noise in manual differentiation in offgas correction and in estimation of heat dissipation.

Culture Dilution Rate ϕ The decreasing weights of the feed medium $W_{\mathsf{feed}}(t)$ and NaOH (pH correction) bottles $W_{\mathsf{NaOH}}(t)$ were monitored, and the total culture dilution rate ϕ was calculated (Fig. S2) from the change of the total weight, the densities ρ_{NaOH}, $\rho_{\mathsf{H_2O}}$, and the set culture volume V_ℓ:

$$\begin{aligned} V(t) =& \frac{W_{\mathsf{NaOH}}(t)}{\rho_{\mathsf{NaOH}}} + \frac{W_{\mathsf{feed}}(t)}{\rho_{\mathsf{water}}} \\ \phi_{\mathsf{raw}}(t) =& -\frac{\mathrm{d}V(t)}{\mathrm{d}t}\frac{1}{V_\ell} \end{aligned} \tag{1}$$

where $\mathrm{d}V(t)$ and $\mathrm{d}t$ were calculated as the means in moving windows of $200\,\mathrm{s}$ (21 measurements). The contribution of pH correction was oscillating, but the amplitude neglibible. The data showed constant feed and only the mean $\phi = \overline{\phi}_{\mathsf{raw}} = 0.089\,\mathrm{h}^{-1}$ was considered in all subsequent calculations.

Period Determination from Dissolved O_2 Oscillation periods $\tau_{osc}(t)$ were calculated from the dissolved O_2 measurement using the `WaveletComp` R package [9] with parameters `loess.span`=0 and `dj`=0.05.

Calculation of $q_{\mathsf{O_2}}$, $q_{\mathsf{CO_2}}$ and RQ The culture temperature $T(t)$, reactor overpressure $P_r(t)$, and partial pressures in the offgas $p_{\mathsf{out}}(t)$ of gases O_2, CO_2 and H_2S were recorded, and metabolic rates calculated after Heinzle [3] but with correction for the delay of offgas measurements [7] in four steps as follows:

Net total mass changes between ingas and offgas were corrected by assuming atmospheric partial pressures p_{in} and no net change in "inert" gases (N_2):

$$\begin{aligned} p_{\mathsf{in,inert}} =& 1 - (p_{\mathsf{in,O_2}} + p_{\mathsf{in,CO_2}} + p_{\mathsf{in,H_2S}}) \\ p_{\mathsf{out,inert}}(t) =& 1 - (p_{\mathsf{out,O_2}}(t) + p_{\mathsf{out,CO_2}}(t) + p_{\mathsf{out,H_2S}}(t)) \\ \hat{p}_{\mathsf{out}}(t) =& p_{\mathsf{out}}(t)\frac{p_{\mathsf{in,\ inert}}}{p_{\mathsf{out,\ inert}}(t)}\ . \end{aligned} \tag{2}$$

The measurements were then corrected for a lag-time of $\tau = 13$ min between culture and measurement device, mostly determined by the head-space volume $V_h \approx 2$ L and aeration rate $\phi_g = 0.15\,\mathrm{L\,min^{-1}}$ as $\tau = V_h \phi_g$, and using a first-order transport equation:

$$p_{\text{culture}}(t) = \hat{p}_{\text{out}}(t) + \tau \frac{\mathrm{d}\hat{p}_{\text{out}}(t)}{\mathrm{d}t}\,, \tag{3}$$

where $\mathrm{d}\hat{p}_{\text{out}}(t)$ and $\mathrm{d}t$ were calculated as the means in moving windows of 200 seconds (21 measurements), resulting in a good match between $p_{\text{culture, O}_2}(t)$ and the measured dissolved O_2 concentration in the culture (Fig. S3).

The total metabolic rates $r(t)$ of the culture were then calculated in $\mathrm{mol\,h^{-1}}$ assuming the ideal gas law:

$$\begin{aligned} \Delta p(t) =& p_{\text{in}} - p_{\text{culture}}(t) \\ P(t) =& P_r(t) + P_0 \\ r(t) =& \phi_g \frac{\Delta p(t) P(t)}{RT(t)}\,, \end{aligned} \tag{4}$$

with the universal gas constant R, atmospheric pressure P_0, the set aeration rate of ϕ_g , and the measured total pressure $P(t)$ and culture temperature $T(t)$.

Specific metabolic rates were calculated by normalizing to the total biomass in the culture:

$$q(t) = \frac{r(t)}{X V_\ell}\,, \tag{5}$$

with biomass concentration X and culture volume V_ℓ. The culture pH was maintained at 3.4 and thus CO_2/bicarbonate buffering in the culture medium is negligible for calculation of q_{CO_2} [3].

The respiratory quotient is the ratio of CO_2 and O_2 turnover rates (excretion and uptake, respectively):

$$\text{RQ}(t) = \frac{q_{\text{CO}_2}(t)}{-q_{\text{O}_2}(t)}\,. \tag{6}$$

The temporal mean over several cycles ($\overline{RQ}$ in Figure 1A are the means of moving windows over 3500 measurements (9.7 h of experiment time).

H_2S Liquid Concentration H_2S had been explored for its potential activity as a synchronizer of the system [12, 6] due to its inhibitory activity on respiratory complex IV, *e.g.*, with reported $K_i = 0.2\,\mu\text{M}$ [13]. Thus, we calculated the liquid concentration C in the culture from the corrected offgas partial pressure $p_{\text{culture}}(t)$, total reactor pressure $P(t)$ and culture temperature $T(t)$ *via* Henry's law:

$$C(t) = p_{\text{culture}}(t) P(t) H^{\ominus} e^{\mathrm{d}H(1/T(t) - 1/T^{\ominus})}\,, \tag{7}$$

with Henry coefficient $H^{\ominus}$ and temperature factor $\mathrm{d}H$ from Sander [10] (Table 1).

Stoichiometric ATP Production Rates $q_{\text{ATP,ox}}$ & $q_{\text{ATP,ferm}}$ ATP production rates of glucose-grown cultures can be estimated from the rates q_{O_2} and q_{CO_2} [16, 15], using the known CO_2 and O_2 stoichiometries of glucose fermentation and oxidation, and experimentally estimated P/O ratios $R_{\text{P/O}} = \frac{\text{ATP}}{\text{O}}$, mol ATP produced per half mol O_2.

Omitting inorganic phosphates and protons for clarity, the overall stoichiometry of complete oxidation of glucose $C_6H_{12}O_6$ in glycolysis, tricarboxylix acid cycle (TCA) and respiration is:

$C_6H_{12}O_6$ + 6 O_2 + 2 ADP + 2 GDP + 12*$R_{P/O}$ ADP $\rightarrow$ 6 CO_2 + 6 H_2O + 2 ATP + 2 GTP + 12*$R_{P/O}$ ATP . (8)

Per mol consumed O_2, metabolism releases 1 mol CO_2, and a respiratory quotient $RQ_{glc} = 1$ indicates purely respiratory use of glucose. Counting GTP as ATP we can summarize the rate of ATP production from complete oxidation of glucose as:

$$q_{ATP,ox,glc} = 2\left(R_{P/O} + \frac{1}{3}\right) q_{O_2} \ , \tag{9}$$

and with a compromise $R_{P/O}$=1 (1.1 in [16], 0.95 in [15] we get a simple scaling $q_{ATP,ox} \approx 2.667 \times q_{O_2}$.

Additional fermentation increases RQ. The overall reaction of glucose fermentation to ethanol (C_2H_6O), again omitting phosphates and protons for clarity, is:

$$C_6H_{12}O_6 + 2\ ADP \rightarrow 2\ C_2H_6O + 2\ CO_2 + 2\ ATP\,, \tag{10}$$

i.e. 1 mol ATP per mol CO_2. Assuming that surplus q_{CO_2} completely stems from additional fermentation, we can subtract the respiratory from the total rate, to estimate the additional ATP production in fermentation:

$$q_{ATP,ferm,glc} = q_{CO_2} - q_{O_2} \ . \tag{11}$$

Fermentation & Ethanol Oxidation. During HOC, the $RQ < 1$ indicates re-uptake and oxidation of the ethanol produced in the preceding LOC phase. The overall stoichiometry of ethanol (C_2H_6O) oxidation has a theoretical $RQ_{etoh} = \frac{2}{3}$:

$$C_2H_6O + 3\ O_2 + 6R_{P/O}\ ADP \rightarrow 2\ CO_2 + 3\ H_2O + 6R_{P/O}\ ATP\,, \tag{12}$$

where 1 ATP lost during the initial reactions of ethanol assimilation is compensated by 1 GTP gained in TCA, and thus:

$$q_{ATP,ox,etoh} = 2R_{P/O,etoh} q_{O_2} \ . \tag{13}$$

Ethanol has a higher degree of reduction (6) than glucose (4) [8], and accordingly Verduyn et al. [15] reported a ≈50% higher P/O ratio on ethanol ($R_{P/O,etoh}$=1.5) than on glucose ($R_{P/O}$=0.95) medium. Assuming this $R_{P/O,etoh}$, we would arrive at a 10–15% higher overall ATP stoichiometry for ethanol re-uptake and oxidation ($q_{ATP,etoh} \approx 3 \times q_{O_2}$) than for glucose oxidation. Assuming complete fermentation and re-uptake and oxidation of the produced ethanol we obtain a lower estimate for glycolytic ATP generation of:

$$q_{ATP,ferm,etoh} = q_{CO_2} - \frac{3}{2} q_{O_2} \ . \tag{14}$$

When assuming, as an extreme alternative scenario, full glycolytic fermentation of glucose to ethanol and ethanol as the sole substrate of respiration, the relative contribution of fermentation to total ATP generation would thus be even lower.

In Figure 1D, $q_{ATP ox}$ and $q_{ATP ferm}$ are the ranges between $q_{ATP ox,glc}$ (lower) $q_{ATP ox,etoh}$ (upper) and $q_{ATP ferm,glc}$ (upper) $q_{ATP ferm,etoh}$ (lower), respectively.

Coarse Estimation of Metabolic Heat Dissipation $\Delta Q'$ Our reactor setup was not optimized for calorimetry as *e.g.* outlined by Marison et al. [5]. Nevertheless, the recorded temperatures of the culture $T(t)$ and the controlling water bath $T_{\mathsf{b}}(t)$, and measured reactor geometry allow a coarse quantitative estimate of the reactor heat dissipation rate $Q'_{\mathsf{tot}}(t)$ in $\mathrm{J\,s^{-1}}$ using Fourier's law:

$$\begin{aligned}\Delta T(t) =& T(t) - T_{\mathsf{b}}(t)\\ Q'_{\mathsf{tot}}(t) =& \frac{\mathrm{d}Q_{\mathsf{tot}}(t)}{\mathrm{d}t} = kA\frac{\Delta T(t)}{\Delta x}\,,\end{aligned} \tag{15}$$

where $k = 1.15\ \mathrm{W\,m^{-1}\,K^{-1}}$ is the heat transfer coefficient of the reactor material (Pyrex glass) [2], and reactor geometry was measured: the thickness of the reactor vessel wall was $\Delta x = 3.2\ \mathrm{mm}$, and the inner surface area of the reactor, in heat exchange with the water bath, was $A = 0.13\ \mathrm{m^2}$.

This heat production includes the technical heat from reactor mixing and aeration, and thus we subtracted the average heat $Q'_{\mathsf{tot},0}$ produced during the starvation phase (at $\phi = 0$ and $q_{\mathsf{O}_2} = 0$, but with aeration and agitation), before onset of the continuous culture feed, and normalized for total biomass, we get:

$$\begin{aligned}\Delta Q'_{\mathsf{tot}}(t) =& Q'_{\mathsf{tot}}(t) - Q'_{\mathsf{tot},0}\\ \Delta Q'(t) =& \frac{\Delta Q'_{\mathsf{tot}}}{XV_\ell}\,.\end{aligned} \tag{16}$$

The mean temperature differences were $\Delta T = 2.36\ \mathrm{K}$ during continous culture (*e.g.* Fig. S1) and $\Delta T_0 = 2.22\ \mathrm{K}$ during the starvation phase, yielding a mean total heat dissipation rate of the culture of $\overline{\Delta Q'}_{\mathsf{tot}} \approx 23.8\,\mathrm{kJ\,h^{-1}}$, and mean specific rate $\overline{\Delta Q'} \approx 4.7\ \mathrm{kJ/h/g_{DCW}}$.

Estimation of Measurement Error Von Stockar *et al.* have used custom-build calorimetric bioreactors [5] to estimate heat dissipation of budding yeast continuous cultures in comparable conditions [1, 17]. They observe a specific heat dissipation per biomass carbon of about 200-220 $\mathrm{kJ/C{\cdot}mol}$. Assuming a carbon content of $C_C = 0.48\,\mathrm{g/g_{DCW}}$ [4, 15, 14], and with the molecular weight of carbon $M_C = 12\,\mathrm{g\,mol^{-1}}$, dilution rate $\phi = 0.089\,\mathrm{h^{-1}}$ and culture volume $V_\ell = 0.635\,\mathrm{L}$, we get a mean heat dissipation per biomass carbon of $\overline{\Delta Q'}\frac{M_c}{\phi V_\ell C_c} \approx 1300\,\mathrm{kJ/C{\cdot}mol}$, *i.e.* $\approx 6\times$ higher.

Alternatively, we can estimate the maximal glucose flux through respiration as 1/6 of the mean total O_2 flux (equ. 4, $\overline{r}_{\mathsf{O}_2}(t) \approx 0.015\,\mathrm{mol\,h^{-1}}$), $r_{\mathsf{Glc,ox}} \approx 0.0025\,\mathrm{mol\,h^{-1}}$, and with $R_{\mathsf{P/O}} = 1$ respiration yields 16 ATP per glucose (equ. 8). Using experimentally established Gibbs free energies of glucose oxidation ($-2872\,\mathrm{kJ\,mol^{-1}}$) and ATP generation ($-51.8\,\mathrm{kJ\,mol^{-1}}$) [18]; this would leave $2872 - 16 \times 51.8 = 2043\,\mathrm{kJ\,mol^{-1}}$ available as heat, while our estimate is $\frac{\overline{\Delta Q'}_{\mathsf{tot}}}{r_{\mathsf{Glc,ox}}} \approx 9369\,\mathrm{kJ\,mol^{-1}}$ (equ. 16), *i.e.* $\approx 4.6\times$ higher. Reaction Gibbs free energies depend on actual concentrations and likely differ (and oscillate) in our system. Nevertheless, the estimates from biomass and glucose flux are at least qualitatively consistent. Due to this uncertainties in our measurements, heat dissipation is only interpreted qualitatively (relative change between starvation, LOC and HOC phases).

Table 1: Physical & Culture Parameters used in calculations.

parameter	symbol	value ± S.D.	note or reference
PHYSICAL			
universal gas constant	R	$8.314\,472\,\mathrm{J\,K^{-1}\,mol^{-1}}$	
standard temperature	$T^{\ominus}$	$298.15\,\mathrm{K}$	
atmospheric pressure	P_0	$101\,325\,\mathrm{Pa}$	
atmospheric partial pressure, O_2	p_{in,O_2}	20.95%	
atmospheric partial pressure, CO_2	p_{in,CO_2}	383 ppm	
atmospheric partial pressure, H_2S	p_{in,H_2S}	0	
Henry coefficient, H_2S	$H^{\ominus}$	$1 \times 10^{-3}\,\mathrm{mol\,m^{-3}\,Pa^{-1}}$	Sander [10]
-"- temperature factor	$\mathrm{d}H$	$2100\,\mathrm{K}$	Sander [10]
density of 10% NaOH at 27° C	ρ_{NaOH}	$1.105\,61\,\mathrm{kg\,L^{-1}}$	`http://www.handymath.com/cgi-bin/naohtble3.cgi`
density of feed medium	ρ_{medium}	$1\,\mathrm{kg\,L^{-1}}$	
REACTOR, static			
culture volume	V_ℓ	$0.635\,\mathrm{L}$	
time delay, offgas measurement	τ	$13\,\mathrm{min}$	
reactor inner surface area	A	$0.132\,217\,9\,\mathrm{m^2}$	
reactor wall thickness	Δx	$3.2\,\mathrm{mm}$	
Pyrex glass heat transfer coefficient	k	$1.154\,784\,\mathrm{W\,m^{-1}\,K^{-1}}$	Carwile and Hoge [2]
REACTOR, calculated			
dilution rate	ϕ	$0.089 \pm 0.003\,\mathrm{h^{-1}}$	
aeration rate	ϕ_g	$0.150 \pm 0.001\,\mathrm{L\,min^{-1}}$	
reactor pressure	P	$101\,707 \pm 102\,\mathrm{Pa}$	
reactor temperature	T	$303.15 \pm 0.04\,\mathrm{K}$	*
water bath temperature	T_b	$300.79 \pm 0.05\,\mathrm{K}$	*
culture pH	pH	3.4±0.1	*
REACTOR, from previous experiments			
biomass, dry cell weight	X	$8\,\mathrm{g_{DCW}/L}$	Sasidharan et al. [11]

*) these values varied with respiratory oscillation (see Text).

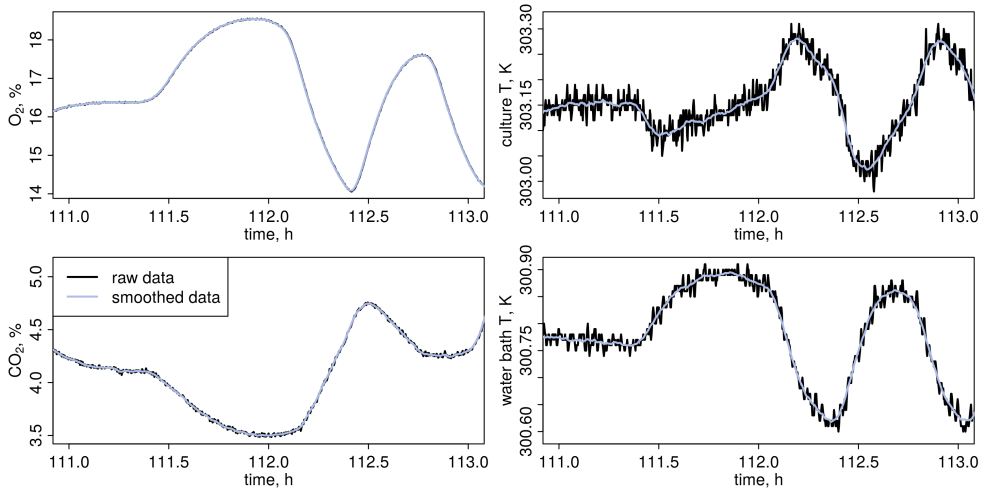

Figure S1: **Raw Data Smoothing.** Offgas partial pressures (left: O_2 and CO_2) were smoothed by a moving average over 10 measurements ($90\,\mathrm{s}$) and culture and water bath temperature (right panels) over 30 measurements ($290\,\mathrm{s}$).

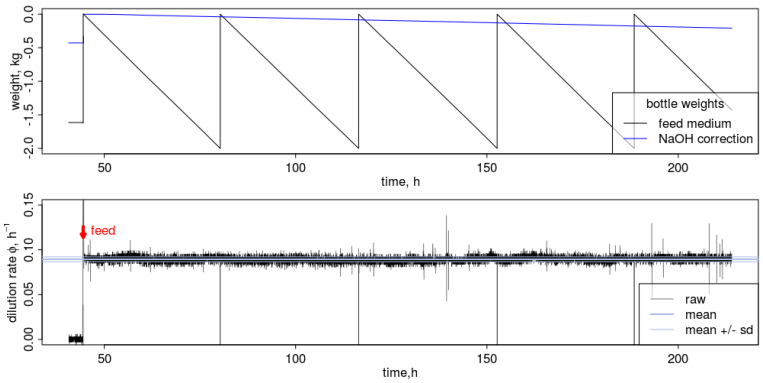

Figure S2: **Calculation of Dilution Rate ϕ.** Upper panel: recorded weights of medium and NaOH correction bottles. The discrete changes stem from attachement of fresh medium bottles. Lower panel: the dilution rate ϕ (black lines) was calculated from the sum of both weights (see Methods). The noise is an artefact of manual differentiation. The global mean (after onset of feed, red arrow at 44.5 h) is the thicker solid blue line, and mean $\pm$ 1 standard deviation (sd) are the thinner blue lines.

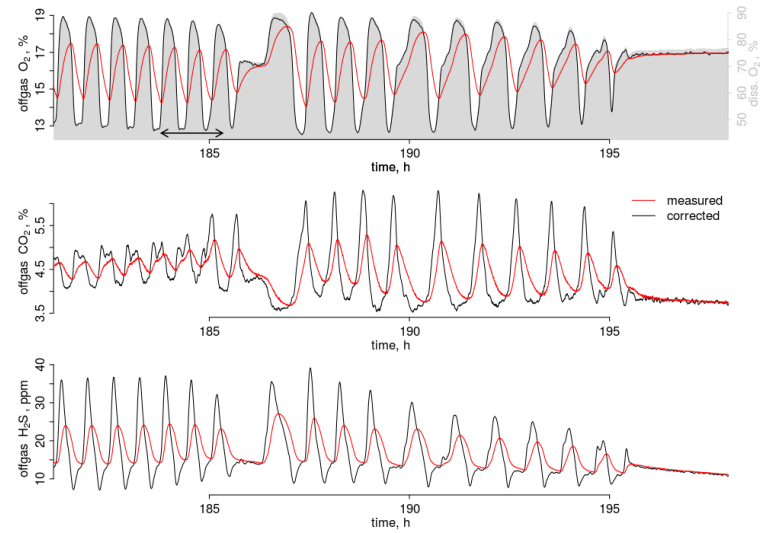

Figure S3: **Offgas Delay Correction.** Measured (red lines: $\hat{p}_{\text{out}}(t)$) and corrected (black lines: $p_{\text{culture}}(t)$) offgas concentrations (see Methods). The gray background in the top panel is the dissolved O_2 concentration (right y-axis), and comparison to corrected offgas data indicates a good match.

References

[1] L.C. Auberson and U. von Stockar. A unified stoichiometric model for oxidative and oxidoreductive growth of yeasts. *Biotechnol Bioeng*, 40(10):1243–1255, Dec 1992.

[2] Lois C Carwile and Harold J Hoge. Thermal conductivity of pyrex glass: Selected values. Technical report, Army Natick Labs Ma Pioneering Research Lab, 1966.

[3] E Heinzle. Mass spectrometry for on-line monitoring of biotechnological processes. In *Biotechnology Methods*, pages 1–45. Springer, 1987.

[4] M. Korhola and K. Edelmann. Yeast preparations enriched with trace elements. *Acta Pharmacologica et Toxicologica*, 59:148–151, 1986. ISSN 1600-0773. doi: 10.1111/j.1600-0773.1986.tb02729.x. URL http://dx.doi.org/10.1111/j.1600-0773.1986.tb02729.x.

[5] I Marison, J-S Liu, S Ampuero, U Von Stockar, and B Schenker. Biological reaction calorimetry: development of high sensitivity bio-calorimeters. *Thermochimica Acta*, 309(1-2):157–173, 1998.

[6] D.B. Murray, R.R. Klevecz, and D. Lloyd. Generation and maintenance of synchrony in *Saccharomyces cerevisiae* continuous culture. *Exp Cell Res*, 287(1):10–5, Jul 1 2003.

[7] D.B. Murray, M. Beckmann, and H. Kitano. Regulation of yeast oscillatory dynamics. *Proc Natl Acad Sci U S A*, 104(7):2241–2246, Feb 2007. doi: 10.1073/pnas.0606677104.

[8] J. A. Roels. Application of macroscopic principles to microbial metabolism. *Biotechnology and Bioengineering*, 22(12):2457–2514, 1980.

[9] A. Roesch and H. Schmidbauer. *WaveletComp: Computational Wavelet Analysis*, 2018. URL https://CRAN.R-project.org/package=WaveletComp. R package version 1.1.

[10] R. Sander. Compilation of Henry's law constants (version 4.0) for water as solvent. *Atmospheric Chemistry and Physics*, 15(8):4399–4981, 2015. doi: 10.5194/acp-15-4399-2015. URL http://www.atmos-chem-phys.net/15/4399/2015/.

[11] K. Sasidharan, C. Amariei, M. Tomita, and D.B. Murray. Rapid DNA, RNA and protein extraction protocols optimized for slow continuously growing yeast cultures. *Yeast*, 29(8):311–322, Aug 2012. doi: 10.1002/yea.2911.

[12] H. Sohn and H. Kuriyama. Ultradian metabolic oscillation of *Saccharomyces cerevisiae* during aerobic continuous culture: hydrogen sulphide, a population synchronizer, is produced by sulphite reductase. *Yeast*, 18(2):125–35, Jan 30 2001.

[13] C. Szabo, C. Ransy, K. Modis, M. Andriamihaja, B. Murghes, C. Coletta, G. Olah, K. Yanagi, and F. Bouillaud. Regulation of mitochondrial bioenergetic function by hydrogen sulfide. part I. biochemical and physiological mechanisms. *Br J Pharmacol*, 171(8):2099–2122, Apr 2014.

[14] P. Van Hoek, J.P. Van Dijken, and J.T. Pronk. Effect of specific growth rate on fermentative capacity of baker's yeast. *Appl Environ Microbiol*, 64(11):4226–4233, Nov 1998.

[15] C. Verduyn, A.H. Stouthamer, W.A. Scheffers, and J.P. van Dijken. A theoretical evaluation of growth yields of yeasts. *Antonie Van Leeuwenhoek*, 59(1):49–63, Jan 1991.

[16] H.K. von Meyenburg. Energetics of the budding cycle of *Saccharomyces cerevisiae* during glucose limited aerobic growth. *Archives of Microbiology*, 66:289–303, 1969. ISSN 0302-8933. doi: 10.1007/BF00414585. 10.1007/BF00414585.

[17] U. von Stockar, Ch. Larsson, I.W. Marison, and M.J. Cooney. Calorimetry of dual limitations in yeast cultures. *Thermochimica Acta*, 250(2):247 – 258, 1995. ISSN 0040-6031. doi: https://doi.org/10.1016/0040-6031(94)02071-U. URL http://www.sciencedirect.com/science/article/pii/004060319402071U. Festschrift Dedicated to Professor Ingolf Lamprecht on the Occasion of his 60th Birthday.

[18] S. Werner, G. Diekert, and S. Schuster. Revisiting the thermodynamic theory of optimal ATP stoichiometries by analysis of various ATP-producing metabolic pathways. *J Mol Evol*, 71(5-6): 346–355, Dec 2010.

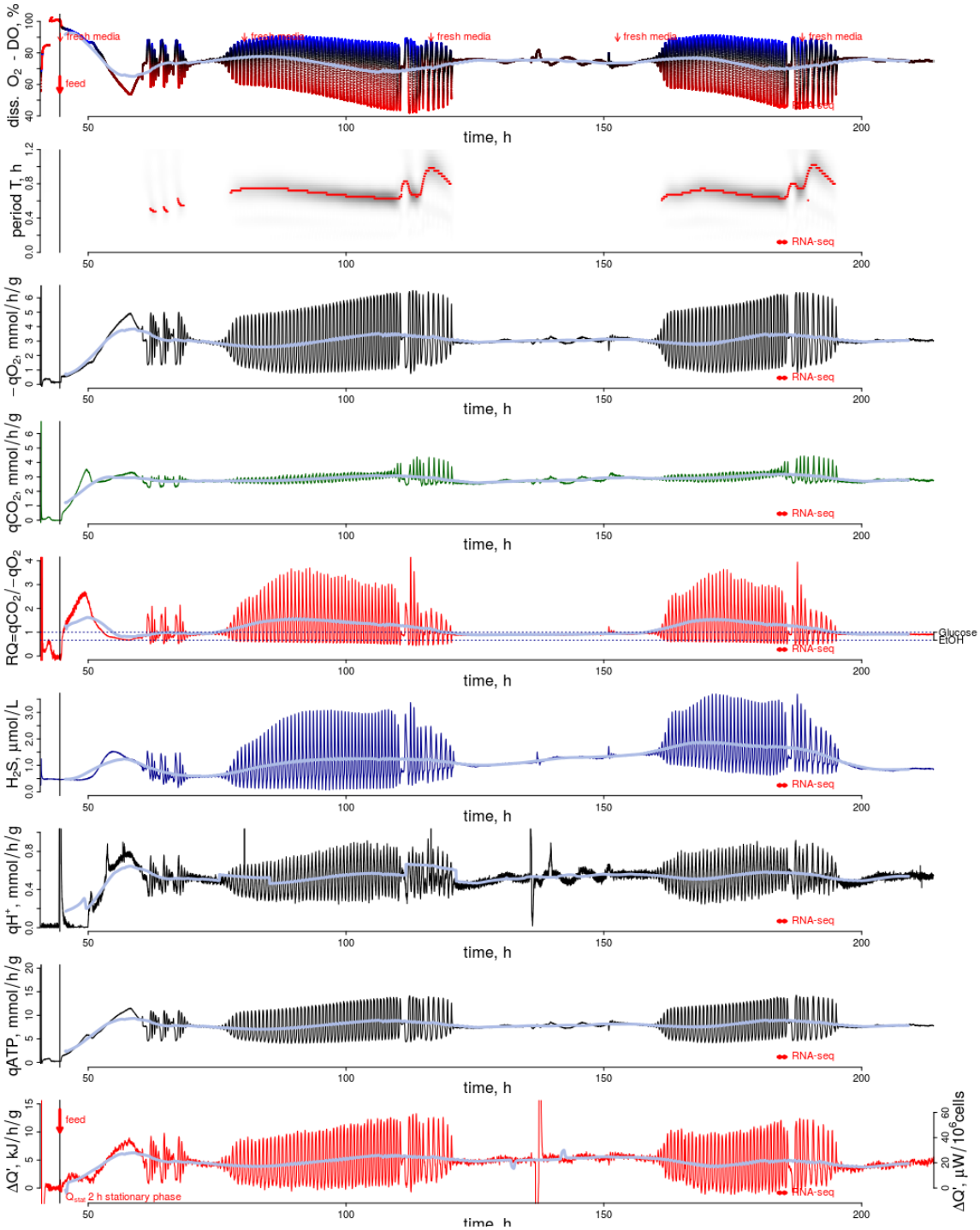

Figure S4: **Culture Dynamics - Time Series.** All data calculated from online measurements (see Methods) over the complete recorded time range, and normalized to $8\,\mathrm{g_{DCW}/L}$ [11]. Red vertical arrows in the top panel indicate the start of continuous culture (feed) and changes of the media bottle (fresh media). The RNAseq experiment range is indicated in all panels by a horizontal arrow.

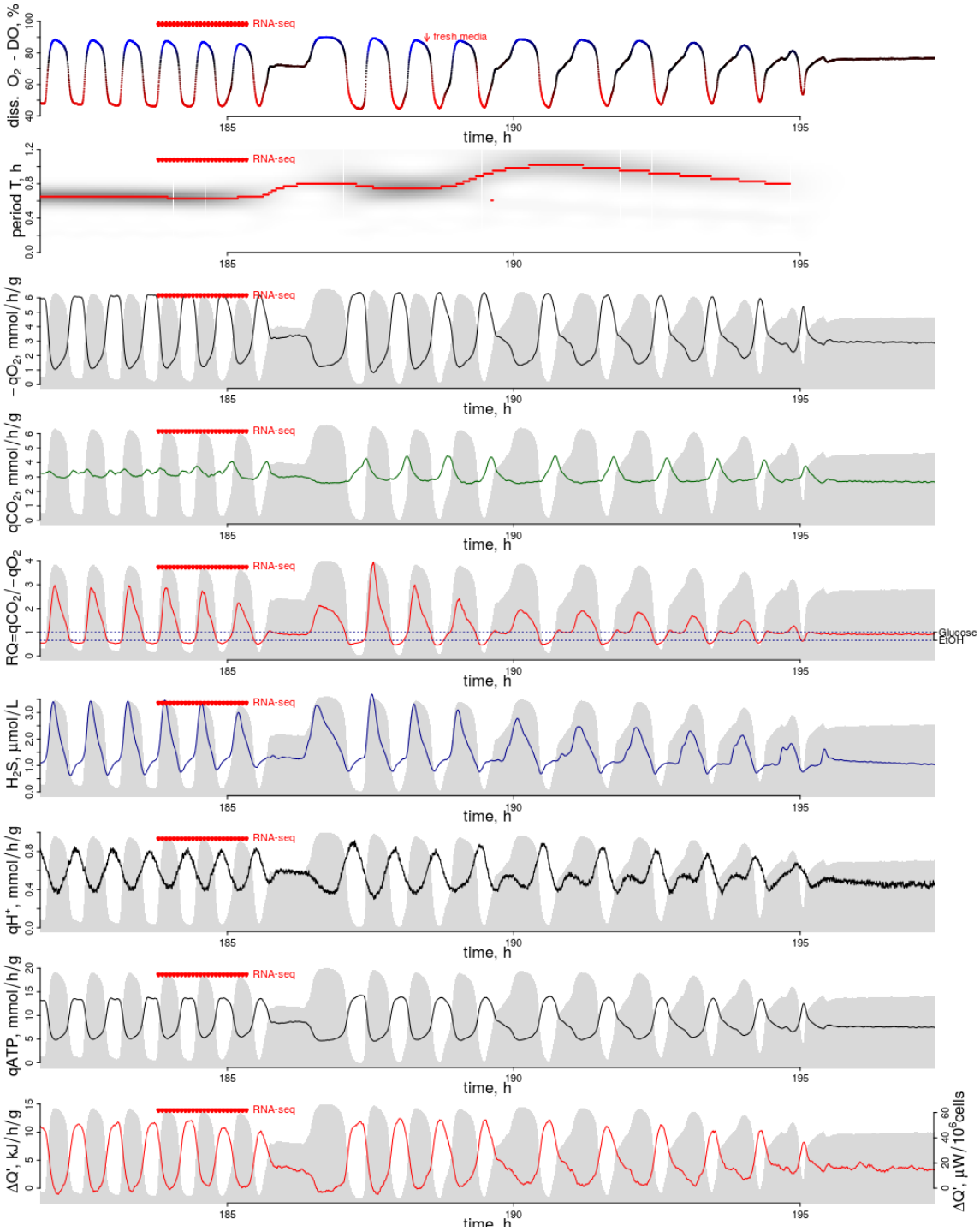

Figure S5: **Culture Dynamics - Time Series.** As Fig. S4 but zoomed in around RNAseq sampling. Each sample is indicated by a vertical arrow.

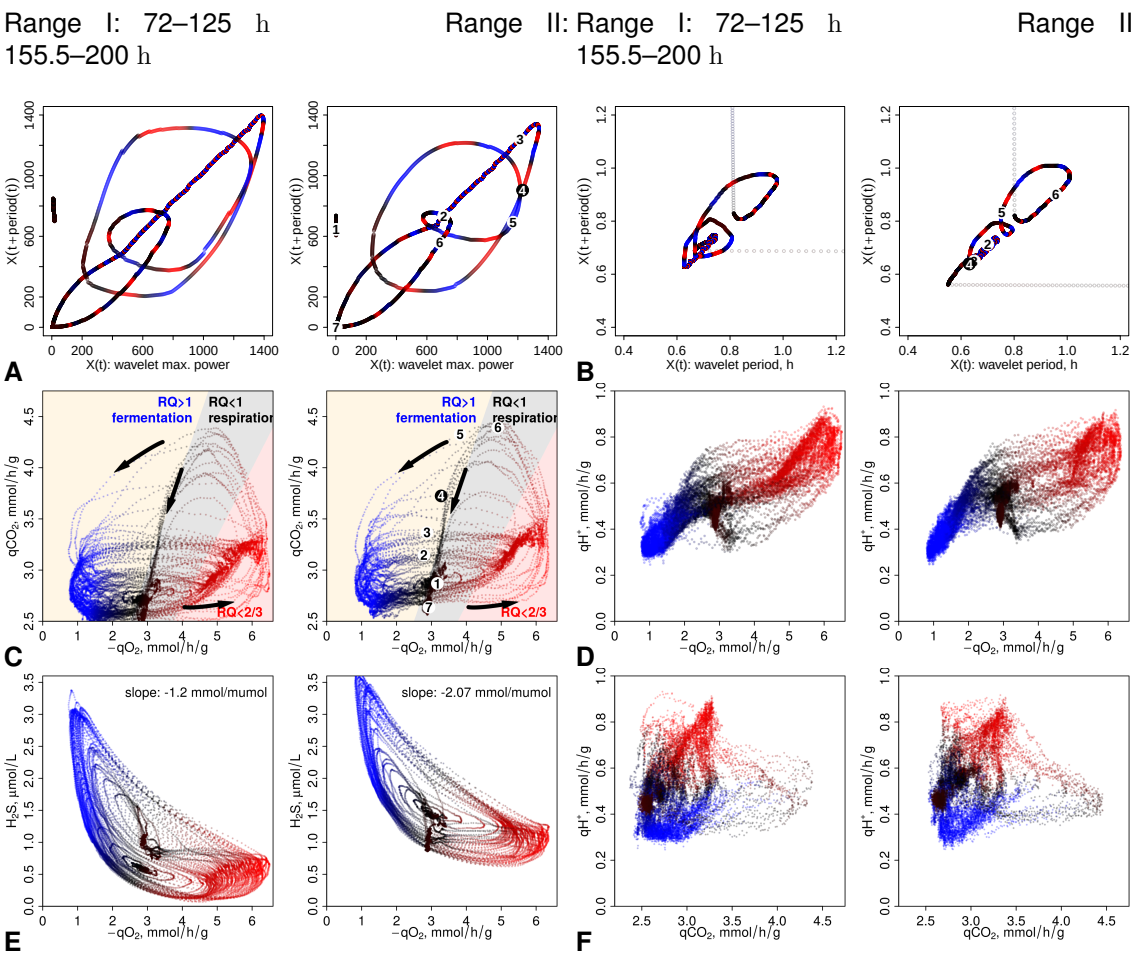

Figure S6: **Poincaré Maps & Phase Portraits** of various culture metabolic rates (Fig. S4 and S5) during the first (left in each panel) and the second (right) instant of the 30-50 h long transients. All data points are colored by the RQ value at the time (panel (B) of q_{CO_2} *vs.* q_{O_2} serves as a legend) and indicate phases of high O_2 consumption (red) and low O_2 consumption (blue). Background colors in the top panels indicate RQ ranges for respiratory (gray and red) and respiro-fermentative metabolism (blue). Bullet points (right panels only) map to their locations in Figure 1 of the main manuscript. Arrows indicate the time direction. All trajectories except q_{CO_2} *vs.* q_{H^+} (right bottom panel) move counter-clockwise. The phase advancement and delays at the bifurcation of system dynamics and the appearance of a novel phase at RQ ≈ 1, as outlined in the main manuscript, are indicated by trajectory points colored in black. **A & B:** Poincaré maps of the maximal power (A) of the wavelet transformed DO data and the period (B) with this power. **C–F:** Phase portraits, each comparing two metabolic rates. **C:** A CO_2 release pulse appears at transition to the RQ ≈ 1 phase. **D:** Phase-advanced proton export. **E:** Phase-delayed H_2S pulse after the RQ ≈ 1 phase. **F:** Uncoupling of q_{CO_2} and q_{H^+}.